J. Membrane Biol. 199, 113–118 (2004)
DOI: 10.1007/s00232-004-0681-z

The Journal of
Membrane
Biology

Optimal-Sensitivity Analysis of Ion Channel Gating Kinetics

A. Kargol[1], **A. Hosein-Sooklal**[2]
[1]Physics Department, Loyola University New Orleans, New Orleans, LA 70118, USA
[2]Department of Physiology and Biophysics, University of Arkansas for Medical Sciences, Little Rock, AR 72205, USA

Received: 23 December 2003/Revised: 25 March 2004

Abstract. We propose a new approach to analysis of kinetic models for ion channel gating, based on application of fluctuating voltages through a voltage clamp, in addition to conventional techniques. We show that the channel kinetics can be probed in a much more sensitive way, leading to more efficient model selection and more reliable estimates of model parameters. We use wavelet transform as an analytic tool for fluctuating currents and parametric dispersion plots as a measure of model compatibility with experimental data.

Key words: Voltage-gated ion channels — Markov models — Nonequilibrium response spectroscopy — Wavelets

Introduction and Theoretical Background

Voltage-gated ion channels are macromolecular assemblies that open ion-selective pores in cell membranes in response to electric fields. They are basic elements behind the electrical excitability of various types of cells and regulate a host of cellular processes (Hille, 2001). A goal of any functional study of ion channels is to develop a mathematical model for the experimental data that reproduces the observed input-output relationships to within some error factor. A majority of reports in the biological literature describe physiological aspects of the channel's behavior and models play only a role in summarizing the experimental data. Much more difficult are studies aimed at determining molecular-kinetic features of the channel-gating mechanism. The gating results from rearrangements of the tertiary structure of channel proteins and models are sought that describe these changes (the number of possible configurational states, voltage-dependence of transition rates, properties of the voltage-sensing mechanism). It is typically assumed that the channel molecule can exist in a small number of discrete states described as closed (C), open (O), or inactivated (I) and representing minima in the molecular "energy landscape". The voltage-dependent forward and backward transition rates between states have the Eyring form: $\alpha_i(V) = \alpha_i(0)\exp(q_i^+ V/kT)$ and $\beta_i(V) = \beta_i(0)\exp(q_i^- V/kT)$, where $\alpha(0)$, $\beta(0)$ are the rates at 0 mV, V is the membrane potential and q_i^+, q_i^- are the (forward and backward) gating charges. The latter are often expressed as $q_i^+ = q_i\delta_i$ and $q_i^- = -q_i(1-\delta_i)$ where q_i is the total gating charge for a given transition and δ_i is the fractional electrical distance. The state occupancy probabilities form a vector $\vec{P}$, evolving according to the master equation:

$$\frac{d\vec{P}}{dt} = \tilde{W}[V]\vec{P} \tag{1}$$

where the transition matrix $\tilde{W}[V]$ consists of the transition rates $\alpha(V)$ and $\beta(V)$.

Attempts at developing general kinetic models have been made for some ion channels, e.g., for the Shaker K^+ channel the leading labs proposed separate and mutually contradictory models (Bezanilla et al., 1994, Zagotta et al., 1994, Schoppa & Sigworth, 1998). For the Na^+ channels the Hodgkin-and-Huxley model (Hodgkin & Huxley, 1952) was a first attempt to develop a picture of ionic conductance in terms of simpler elements, and although not formulated in these terms, it was equivalent to a Markov model. These reports, however, led to a certain amount of skepticism as to a complete viability of the goal of developing a comprehensive Markov model that reflects molecular-kinetic features of the channels, based only on currently available experimental data. It is widely acknowledged that all existing models are incomplete, ambiguous, and describe only certain features of channel behavior.

Correspondence to: A. Kargol; email: akargol@loyno.edu

One source of these ambiguities is our inability to directly measure most of the kinetic variables and a limited "resolution" of current recordings. The vast majority of the experimental data is obtained using a voltage-clamp technique (Hille, 2001) in which current transients following a given applied voltage are measured. Originally developed to measure the macroscopic ionic currents, the voltage clamp technique has been modified (Sakmann & Neher, 1995) to include single-channel recordings (taken from small membrane patches containing single channels) and gating currents (reflecting movement of charged residues in channel proteins). While the ionic currents are most efficient in resolving the transitions between open states and the nearest closed states, the gating currents contain contributions from all voltage-dependent transitions, but suffer from mixing of signals from different transitions. There is also a more fundamental source of ambiguity in kinetic modeling that has been attributed to the nature of currently used voltage-clamp protocols (Millonas & Hanck, 1998a, 1998b; Kargol et al., 2002). Despite all the refinements, the basic philosophy behind all ion-channel experimentation is the same: the membrane voltage is changed stepwise at only few discrete times and the resulting relaxation transients are recorded. This response is due to a redistribution of state occupancies as the ensemble relaxes back to equilibrium. Although such near-equilibrium studies may seem the most appropriate to test physiological responses of channels, they are hardly sufficient to discover all molecular-kinetic aspects of gating (Millonas & Hanck, 1998a, 1998b).

We use a novel method in electrophysiology, the nonequilibrium response spectroscopy (NRS), proposed recently (Millonas & Hanck, 1998a, 1998b, Kargol et al., 2002) to target such modeling ambiguities. It involves application of high frequency voltage waveforms through a voltage clamp. An ensemble of channels subjected to NRS fluctuating potentials can be driven into states arbitrarily far from the equilibrium manifold (Millonas & Hanck, 1998a, 1998b) and areas of the kinetic manifold unreachable by traditional methods can be explored. If the voltage fluctuation frequency interacts with the time scales of the channel kinetics, the response becomes very sensitive to subtle details of the kinetic model. Hence, new information can be gained and the resulting experimental data puts new constraints on the kinetic models (Millonas & Hanck, 1998a, 1998b, Kargol et al., 2002).

The nonequilibrium response spectroscopy has been described in detail in previous publications (Millonas & Hanck, 1998a, 1998b; Hosein-Sooklal & Kargol, 2002; Kargol et al., 2002). For the sake of completeness we present below a brief summary of the method. We proposed two types of NRS protocols (Kargol et al., 2002): the ensemble and the single-pulse protocols. The former are based on repeated applications of voltage waveforms from a certain statistical ensemble. Following Millonas and Hanck (1998a, 1998b) we used the dichotomous noise (DN). The dichotomous noise consists of random voltage fluctuations between two values. It is characterized by these two voltage values, the switching frequency and the temporal asymmetry (i.e., the percentage of time spent in either of the two voltage extremes). Since the DN is a Markovian (memoryless) stochastic process itself, its effect on ion channel gating kinetics can be modeled by incorporating it into the channel kinetic scheme, as shown in Millonas and Hanck (1998b). The probability distribution vector for this expanded model evolves according to the double-dimensional conditional master equation.

The single-pulse protocols involve only few fluctuating voltage pulses designed specifically to probe particular aspects of channel kinetics. We developed an algorithm for constructing waveforms with particular temporal and spectral properties in a wavelet basis (Kargol et al., 2002). The wavelet analysis is a relatively new tool and has been applied to a variety of problems including signal analysis, image compression and denoising, etc. The idea of wavelet analysis is similar to the Fourier analysis. The difference is that in the latter case the analyzing trigonometrical functions have infinite support (thus providing detailed spectral information, but virtually no temporal information about the signal) and wavelets have finite supports (yielding simultaneous spectral and temporal information). While typical use of wavelets is for signal analysis, we employed them to synthesize a waveform with desired properties. In particular, we used the dyadic wavelet basis consisting of functions of the form:

$$\psi_{m,n} = 2^{-m/2}\Psi(2^{-m}t - n) \tag{2}$$

where Ψ is the so-called mother wavelet. Indices m and n are referred to as the dilation and translation indices. The dilation index determines what range of frequencies the function $\psi_{m,n}$ possesses and the translation index points to when these frequencies are "turned on and off". In general, by taking a superposition of such wavelets $f(t) = \sum_{m,n} d_{m,n}\psi_{m,n}$ and adjusting the coefficients $d_{m,n}$, we can construct a function with arbitrary spectral and temporal properties. Our strategy for voltage waveform design is an optimization procedure where such a superposition of wavelets is sought to maximize a cost-functional dependent on specific goals. If the aim is to determine the best of model topologies proposed for a given channel we use the *model sensitivity* defined simply as the χ^2 error between model responses to a given voltage protocol: $S_m = \sum_t (i_1(t) - i_2(t))^2$. The model response is the solution to the master equation (Eq. 1), but since in this case the voltage (and henceforth the

transition matrix) became time-dependent, the solution was found numerically by iteration (Hosein-Sooklal & Kargol, 2002, Kargol et al., 2002). Once the optimal topology is found, we aim to precisely determine the model transition rates using the notion of *parametric sensitivity* (Kargol et al., 2002). It is defined as the change in model response (the occupation probabilities or currents, ionic or gating) caused by a small variation in model parameters. For instance, the experimentally observable quantity $\Pi[\alpha](t)$ can be the macroscopic ionic current, proportional to the projection $\vec{O}$ of the probability vector $\vec{P}$ onto the open states: $\Pi[\alpha](t) = \vec{O} \cdot \vec{P}[\alpha](t)$, where α is a generic name for one of the model parameters. The sensitivity in parameter α is defined as:

$$S_\alpha(t) = \frac{1}{\delta\alpha}\left[\int_0^t ds(\Pi[\alpha+\delta\alpha](s) - \Pi[\alpha](s))^2\right]^{1/2} \qquad (3)$$

where $\delta\alpha$ is a small parameter variation. The sensitivity can be computed for each kinetic parameter independently or jointly. In the latter case, the sensitivity is directionally nonuniform in parameter space. Typically, there are well defined manifolds along which the sensitivity gradient is the least steep. Joint variation of parameters along this manifold is not easily detectable by currently used experimental protocols.

Materials and Methods

We recorded macroscopic ionic currents from human cardiac Na^+ channels (hH1A) stably expressed in HEK293 cells. The details of cell preparation, recording techniques and solutions were as described in Hosein-Sooklal and Kargol (2002). The main issue in current recordings was the bandwidth of the recording apparatus. It had to be large enough to accomodate fluctuating voltage waveforms. We used fire-polished borosilicate pipettes to minimize the input RC time. Only data with the RC time less than 20 μs (bandwidth of 8 kHz) were used.

For comparison with experimental data, the macroscopic ionic currents have been modeled as: $i(t) = g_0 g(V)(V - V_r)\vec{O} \cdot \vec{P}(t)$ where V_r is the reversal potential, $g(V)$, the nonlinear part of the membrane conductance, both of which can be found in separate experiments (Kargol et al., 2002, Millonas & Hanck, 1998b), and g_0, a scaling factor related to the expression level of a particular cell. The procedure for finding the probability vector $\vec{P}(t)$ for channels driven by the DN has been described in Millonas and Hanck (1998a, 1998b). For the time-dependent voltage pulses $V(t)$, the formal solution to the master equation can be written as: $\vec{P}(t) = \exp\left(\int_0^t ds\tilde{W}[V(s)]\right)\vec{P}(0)$. The initial probability distribution $\vec{P}(0)$ is determined by the holding potential V_h, and the explicit form of $\vec{P}(t)$ we found by iteration (Kargol et al., 2002). All programs for pulse design, data analysis and modeling were written in Matlab (Mathworks, Natick, MA).

Results and Discussion

We considered two models for the Na^+ channels: the Vandenberg-Bezanilla (VB) (Vandenberg & Bezanilla, 1991) and the Millonas-Hanck (MH) model

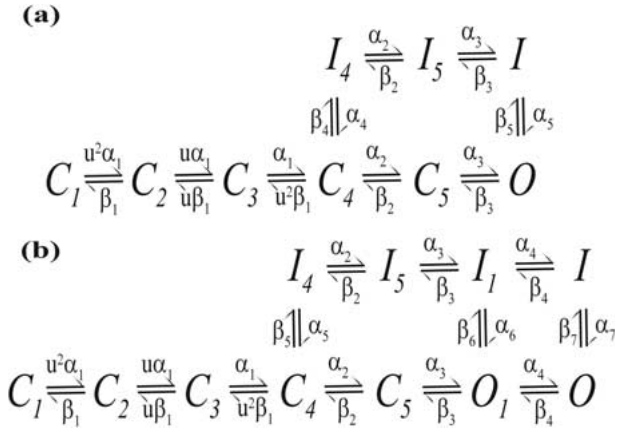

Fig. 1. Kinetic models for the K^+ channels. (*a*) the VB model (Vandenberg & Bezanilla, 1991) developed for the neural isoform of the K^+ channel. This topology has been used also for the cardiac isoform. (*b*) the MH model (Millonas & Hanck, 1998a).

(Millonas & Hanck, 1998b) (Fig. 1). Both attempt to capture main features of current recordings: a delay in channel openings due to several states in the activation pathway and spontaneous inactivation resulting from weakly voltage-dependent transitions to inactivated states. The difference is in the number of open states. Initially, both models were fit to a typical set of stepped voltage protocols, including the activation (steps from a holding voltage of −130 mV to a series of voltages starting from −122 mV in 8 mV increments) and tail series (depolarizing prepulse to 32 mV for 1 mV followed by steps to values from −150 mV in 12 mV increments). The values of model parameters have been reported in Hosein-Sooklal and Kargol (2002). Since both models reproduce this type of data equally well, no conclusion regarding the number of open states can be drawn.

We implemented our pulse-design algorithm (Kargol et al., 2002) to get voltage waveforms that maximize the model sensitivity. We used the dyadic basis of Daubechies 8 wavelets $\psi_{m,n}(t) = 2^{-m/2}\Psi(2^{-m}t - n)$, where $\Psi(t)$ is the mother wavelet (Daubechies, 1992). An initial pulse was constructed as a random superposition of wavelets $V(t) = \sum_{m,n} d_{m,n}\psi_{m,n}(t)$, typically with 7–8 wavelet multiresolution levels (i.e., frequency content of the pulse up to 6–8 kHz). The algorithm was a random search in parameter space for the values of coefficients $d_{m,n}$ that maximize the model sensitivity S_m. Because of the random nature of this algorithm, each run resulted in a different waveform. We have constructed several pulses with maximal fluctuation amplitudes limited only by the cells' expected ability to withstand such voltage fluctuations. For each of the pulses, the model currents were compared with ionic currents measured from the hH1A channels. Data presented in this paper is a continuation of our previous work (Hosein-Sooklal & Kargol, 2002). In the previous

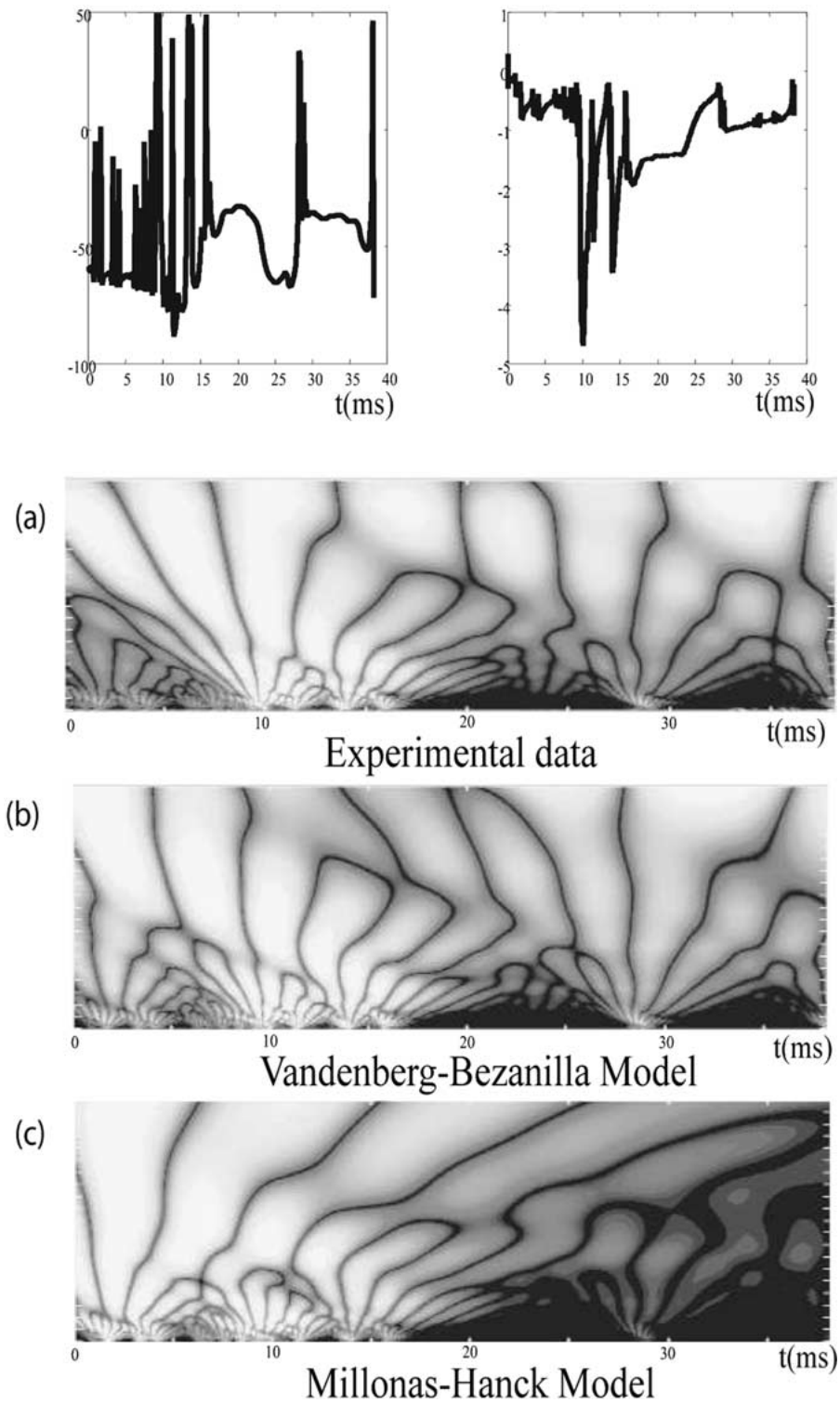

Fig. 2. Sample response to single-pulse protocols. The voltage pulse (*top left*) and ionic current response (*top right*) are shown. Voltage is measured in mV and the corresponding currents in nA. We compared continuous wavelet transforms of the experimental data (*a*), the VB (*b*) and the MH (*c*) model currents. The plots show spectro-temporal patterns in the data. The horizontal axis represents the time during the signal (0–40 ms for pulses used in our experiments). The vertical axis shows the wavelet levels. They are related to the frequency content of the signal with the lowest frequencies at the top and the highest at the bottom. The absolute values of the wavelet transform coefficients are plotted on a grey scale. Dark areas correspond to near-zero values of the coefficients and the bright areas, to their large values. The significance of bright areas is that at these times (read on the horizontal axis) specific frequencies (determined by the coordinate on the vertical axis) dominated the signal.

paper we used the discrete wavelet transform, while here, for easier comparison of fluctuating signals, we implemented the continuous wavelet transform that better uncovers spectro-temporal patterns in the data. Sample data for the voltage pulse with amplitude 140 mV are shown in Fig. 2. The upper left panel in that figure shows the voltage waveform obtained from our pulse-design algorithm for maximal model sensitivity. The voltage was applied for 40 ms and the values given are in mV. The upper right panel is the corresponding ionic current, in nA. The remaining three panels are the continuous wavelet transforms of the experimental data (*a*), the VB-model current (*b*) and the MH-model current (*c*). This gray-scale figure

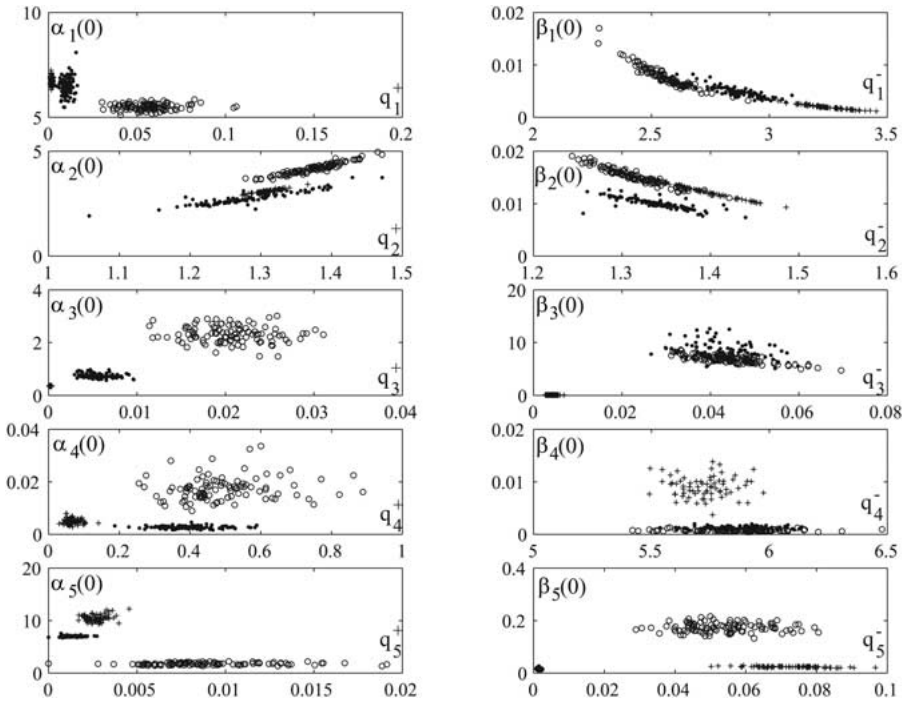

Fig. 3. Dispersion plots for the model parameters in the VB model. Each panel is a different section of the model parameter space and each dot represents a result of one run of the fitting algorithm. We used ionic current for: 1. stepped voltage (o), 2. DN (●), and 3. single-pulse protocols (+). $\alpha_i(0)$ and $\beta_i(0)$ in [ms^{-1}], q_i in units of e.

shows the absolute values of the wavelet expansion coefficients $d_{m,n}$. The wavelet levels labeled by the dilation index m increase along the vertical axis and are related to the frequency content of the signal—with the highest frequencies at the bottom. The translation index n (labeling when in the signal given frequencies are present) is plotted on the horizontal axis. The dark areas represent small (near-zero) values of the wavelet expansion coefficients. It can be noticed that while the VB model reproduces the experimental data well, the MH model overestimates the rate of inactivation. Namely, the values of expansion coefficients decrease in time (i.e., to the right in the gray-scale plots) much faster for the MH model than for the experimental data. The overall spectro-temporal pattern for the MH-model current also visually differs from the experimental data. A similar trend has been noticed for other pulses. This is an argument against the inclusion of the second open state in the model or at least against its direct link to the inactivation pathway.

Hence, we further considered only the VB model and applied the optimal parametric sensitivity pulses to improve parameter estimates. For instance, preliminary fits to stepped voltage data resulted in the following parameter values for transition rate α_5: $\alpha_5(0) = 1.77$ ms^{-1}, $q_5 = 0.063$e and $\delta_5 = 0.1853$, where $q^+{}_5 = q_5\delta_5$, $q^-{}_5 = -q_5(1-\delta_5)$; is the total gating charge and δ_5, the fractional electrical distance for this transition. We have constructed pulses that maximize the joint sensitivity in parameters $\alpha_5(0)$ and q_5. The observed increase in sensitivity was by a factor of 2 ($\alpha_5(0)$) or 9 (q_5).

The model-fitting algorithm is a version of the simulated annealing method, i.e., a random search in the parameter space with a decreasing search radius (Millonas & Hanck, 1998b, Kargol et al., 2002). Because of its random nature each run of the algorithm resulted in a different set of model parameters. The dispersion of these values and their location in parameter space are a reflection of the parametric sensitivity. We ran the program 100 times each for three different sets of experimental data: 1) the stepped voltage protocols, 2) stepped and DN protocols (random voltage switching between −120 mV and −30 mV with frequencies 0.7, 1, 2, 3, 5 and 8 kHz), and 3) stepped and single-pulse protocols (maximal sensitivity pulses with peak-to-peak amplitudes of 140, 180 and 200 mV). The results are shown in Fig. 3 where different symbols correspond to the three sets of data. We included only the parameter sets with the same χ^2 error cutoff, normalized to the number of sweeps and the sampling rate. For transition rates α_1/β_1, α_2/β_2 and to a lesser extent α_4/β_4, there is an overlap, indicating that all three methods yield similar parameter values. In case of α_5/β_5, as well as α_3/β_3, each set of data gives a distinctly different set of model parameters. For data set (2) we got $\alpha_5(0) = 6.98$ ms^{-1}, $q_5 = 0.0029$e, while for set (3), $\alpha_5(0) = 10.63$ ms^{-1} and $q_5 = 0.068$e. Numerical experiments (Kargol et al., 2002) with simulated experimental data (data computed using a known model) show that if the correct model topology is fit to it there is always an overlap and only the size of the parameter dispersion can be reduced using

additional data sets. The differences in parameter values observed in Fig. 3 show that the VB model, even if apparently superior to the MH model, is not fully compatible with the NRS experimental data either and a better model ought to be sought. Hence the optimal sensitivity NRS method not only yields more reliable parameter values but also can be a test of adequacy of model topology. Such non-overlapping clustering of model parameters in dispersion plots indicates that the model topology used is not fully compatible with experimental data. Results reported here use macroscopic ionic currents only but we expect the method to be more efficient with gating currents.

Models of ion channel kinetics are hypotheses, subject to experimental verification. Model refinement is achieved by introducing more types of data or by increasing the number of voltage protocols. We introduced new types of protocols, fundamentally different from currently used ones. They are very efficient in model selection and can be used to reject or modify models in cases where standard relaxation transient methods fail. The dispersion plots can directly show incompatibility of proposed models with the experimental data. The NRS technique is an application of fluctuation-induced phenomena to ion channel gating kinetics but it can also be used to aid model selection and analysis in other areas of physics, chemistry, or biology, where similar phenomena are observed and the kinetics described by the master equation.

References

Bezanilla, F., Peroso, E., Stefani, E. 1994. Gating of Shaker K^+ channels II: the components of gating currents and a model of channel activation. *Biophys. J.* **66:**1011–1021

Daubechies, I. 1992. Ten Lectures on Wavelets. SIAM, Philadelphia, PA

Hille, B. 2001. Ionic Channels of Excitable Membranes. 3rd ed. Sinauer Associates Inc., Sunderland, MA

Hodgkin, A.L., Huxley, A.F. 1952. A quantitative description of membrane current and its application to conduction and excitation in nerve. *J. Physiol.* **117:**500–544

Hosein-Sooklal, A., Kargol, A. 2002. Wavelet Analysis of Non-equilibrium Ionic Currents in Human Heart Sodium Channel (hH1a). *J. Membrane Biol.* **188:**199–212

Kargol, A., Smith, B., Millonas, M.M. 2002. Applications of nonequilibrium response spectroscopy to the study of channel gating. Experimental design and optimization. *J. Theoret. Biol.* **218:**239–258

Millonas, M.M., Hanck, D.A., 1998a. Nonequilibrium response spectroscopy and the molecular kinetics of proteins. *Phys. Rev. Lett.* **80:**401–404

Millonas, M.M., Hanck, D.A. 1998b. Nonequilibrium response spectroscopy of voltage-sensitive ion channel gating. *Biophys. J.* **74:**210–229

Sakmann, B., Neher, E. 1995. Single Channel Recording. Plenum, New York. *Biophys. J.* **74:**210–229

Schoppa, N.E., Sigworth, F.J. 1998. Activation of Shaker potassium channels I. Characterization of voltage-dependent transitions. *J. Gen. Physiol.* **111:**271–294

Vandenberg, C.A., Bezanilla, F. 1991. A sodium channel gating model based on single channel, macroscopic ionic and gating currents in the squid giant axon. *Biophys. J.* **60:**1511–1533

Zagotta, W.N., Hoshi, T., Aldrich, R.W. 1994. Shaker potassium channel gating III: evaluation of kinetic models for activation. *J. Gen. Physiol.* **103:**321–362